Int J Thermophys (2008) 29:1385–1394
DOI 10.1007/s10765-008-0471-4

Trilobal Polyimide Fiber Insulation for Cryogenic Applications

M. Geisler · J. Wachtel · F. Hemberger · T. Schultz · S. Vidi · H.-P. Ebert

Received: 4 October 2007 / Accepted: 9 June 2008 / Published online: 25 June 2008

Abstract Recent measurements have shown a record-breaking low thermal conductivity λ_{total} of less than $0.25 \times 10^{-3}\,\text{W}\cdot\text{m}^{-1}\cdot\text{K}^{-1}$ at temperatures of 120 K for an evacuated sample consisting of polyimide fibers with a trilobal fiber cross section. Existing models for the heat transport in fiber insulations cannot sufficiently describe fiber insulations consisting of fibers with non-cylindrical cross sections. In this article, a modification for the model for cylindrical fibers will be presented. The modifications for the trilobal cross section of the fiber will be explained and compared to the original cylindrical model. The results of the theoretical calculations will be discussed in comparison to experimental results of measurements performed with a guarded hot-plate apparatus at temperatures in the range from 120 K to 420 K.

Keywords Contact radius · Cryogenic insulation · Fiber model · Fibrous insulation · Polyimide · Thermal conductivity · Trilobal · Unit cell

1 Motivation and Classification

The best insulation for a cryogenic application needs to fulfill many requirements. For example, processing, maintenance, mechanic stability, handling, costs, aging, disposal, health hazard, load- and temperature cycling, temperature endurance, gas pressure resistance, etc., and, of course, thermal conductivity are the properties of interest.

M. Geisler (✉) · J. Wachtel · F. Hemberger · S. Vidi · H.-P. Ebert
Functional Materials for Energy Technology, Bavarian Center For Applied Energy Research (ZAE Bayern), Am Hubland, 97074 Wurzburg, Germany
e-mail: geisler@zae.uni-wuerzburg.de

T. Schultz
Process Technology & Engineering, Evonic Industries AG, Rodenbacher Chaussee 4, 63457 Hanau-Wolfgang, Germany

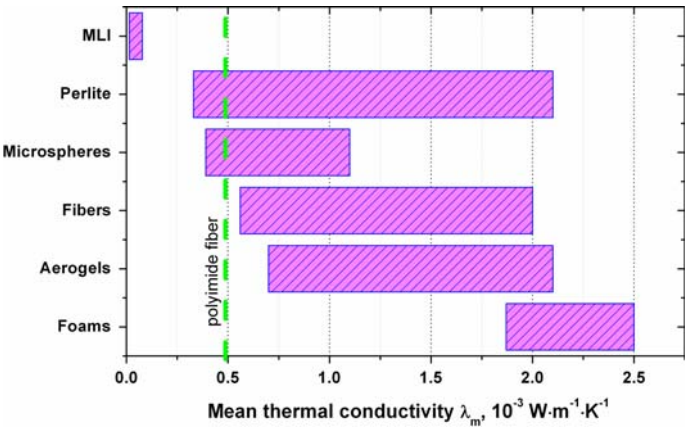

Fig. 1 Comparison of the mean thermal conductivity of insulation materials for a typical temperature difference in cryogenic application with $T_{\text{cold}} = 77\,\text{K}$ (LN_2) and $T_{\text{hot}} = 300\,\text{K}$ (ambient temperature). A spread in the measured values (data from literature) for each material is shown. The dashed line represents the calculated mean thermal conductivity of a cryogenic insulation made of polyimide fibers

Thus, making a choice for the proper insulation material does not necessarily result in the insulation with the lowest thermal conductivity. Fiber insulations have a long history in low-temperature applications [1–3]. The main advantage of fibrous insulation is their easy handling compared to insulations made of granular or powder and insulations based on heat shields (MLI—multilayer insulation).

The mean thermal conductivity λ_{m} of a thermal insulation is defined as

$$\lambda_{\text{m}} = \frac{1}{T_{\text{hot}} - T_{\text{cold}}} \int_{T_{\text{cold}}}^{T_{\text{hot}}} \lambda(T)\mathrm{d}T. \tag{1}$$

In Fig. 1 a comparison of the mean thermal conductivity of typical materials for cryogenic insulations can be found. The shown values are valid for an evacuated insulation with a surface temperature of $T_{\text{cold}} = 77\,\text{K}$ (LN_2) and $T_{\text{hot}} = 300\,\text{K}$. One of the lowest measured thermal conductivity for an evacuated fiber insulation was about $0.6 \times 10^{-3}\,\text{W}\cdot\text{m}^{-1}\cdot\text{K}^{-1}$. The mean fiber diameter of this optimized insulation was $1.143\,\mu\text{m}$ [4]. The trilobal polyimide fibers investigated in this work have a record breaking low thermal conductivity for fibrous insulations. The calculated mean thermal conductivity $\lambda_{\text{m}} = 0.48 \times 10^{-3}\,\text{W}\cdot\text{m}^{-1}\cdot\text{K}^{-1}$ (dashed line, Fig. 1) is significantly lower than the thermal conductivity of the standard fiber insulations.

In Fig. 2 an image of the investigated fiber insulation, taken with a scanning electron microscope, is shown. The predominant cross-sectional shape with the characteristic three arms is called trilobal. This typical cross-sectional shape is assumed to be the major reason for the low thermal conductivity of the investigated fibrous insulation. But there is even a remaining potential for the optimization of this material. For example, the fiber diameter could be modified to minimize the thermal conductivity caused

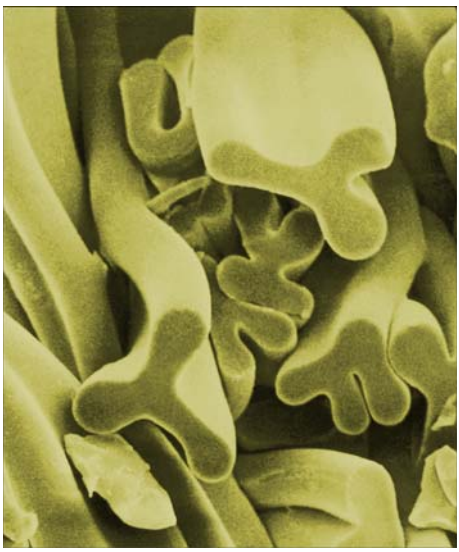

Fig. 2 Picture taken with a scanning electron microscope. The cross section of the fiber is irregularly lobed. Predominant among other fibers cross sections is the three-armed (trilobal) cross section. The titer of the fiber is 2.2 dtex (radius $\sim 7\,\mu$m)

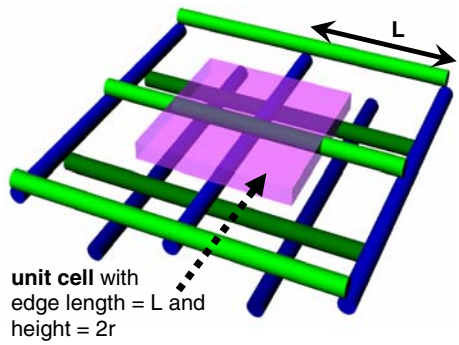

Fig. 3 Theoretical model for fiber insulations consists of layers of parallel fibers with cylindrical cross section and with equidistant spacing L. For heat transport calculations in fibrous media, a unit cell (box depicted) is needed

by the solid structure, or one could be adding infrared opacifiers to reduce the heat transfer caused by radiation.

2 Model

The functional principle of all fiber insulations is to enlarge the path that heat has to travel from the warm side to the cold side. The calculation of the effective thermal conductivity of the fiber matrix λ_{solid} is based on a fiber model by [3]. The model consists of layers of parallel fibers with cylindrical cross section and with equidistant spacing L. The following layer is perpendicular and shifted $L/2$ to the prior. In the same way, the entire insulation can be built up and described physically (Fig. 3).

For thermal calculations, just one representative unit cell is needed. The box in Fig. 3 depicts the chosen unit cell with a length L and height $2r$ (r being the radius). One fiber element of the length L is located in the center of the unit cell. The total thermal

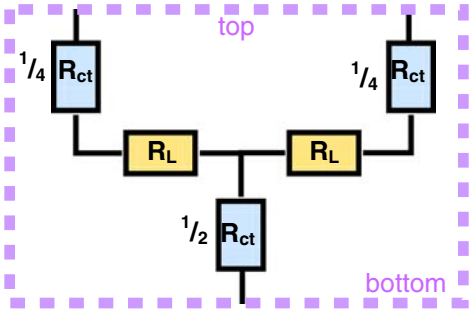

Fig. 4 Schematic resistance network of the unit cell

resistance R_{total} is determined by the conductor-resistance R_{L} and contact-resistance R_{ct} of the fiber:

$$R_{\text{total,uc}} = \frac{1}{2}R_{\text{L}} + \frac{5}{8}R_{\text{ct}}. \tag{2}$$

A schematic resistance diagram of the chosen unit cell is depicted in Fig. 4 [3, 5, 6].

The conductor-resistance R_{L} and the contact-resistance R_{ct} for the chosen unit cell are

$$R_{\text{L}} = \frac{L/2}{\pi r^2 \lambda_{\text{bulk}}}, \tag{3}$$

and

$$R_{\text{ct}} = \frac{1}{2a_{\text{ct}}\lambda_{\text{bulk}}}, \tag{4}$$

where a_{ct} is the Hertzian contact radius [7]. For perpendicular orientated fibers, it is given by

$$a_{\text{ct}} = \sqrt[3]{\frac{3}{2}\frac{1-\nu^2}{E_{\text{mod}}}Fr}, \tag{5}$$

where ν is the Poisson's ratio, E_{mod} is the elastic modulus, F is the average force on one contact point, and r is the fiber radius.

Finally, the total thermal resistance of the unit cell, $R_{\text{total,uc}}$, and the corresponding solid thermal conductivity λ_{solid} can be described by

$$R_{\text{total,uc}} = \frac{1}{4}\frac{L}{\pi r^2 \lambda_{\text{bulk}}} + \frac{5}{16}\frac{1}{a_{\text{ct}}\lambda_{\text{bulk}}} \text{ and} \tag{6}$$

$$\lambda_{\text{solid}} = \frac{2r}{L^2\ R_{\text{total,uc}}}. \tag{7}$$

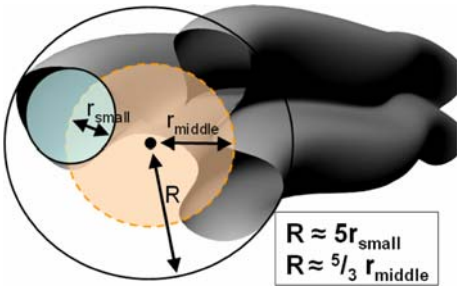

Fig. 5 Diagram of the trilobal fiber for the different radii used in the adapted fiber model

Moreover, a relationship between the density of the sample ρ and the density of the bulk material ρ_0 can be derived regarding the ratio of the unit cell volume V_{uc} and the real fiber volume V_{fiber}. Thus, the functional relationship among L, ρ, ρ_0, and r is

$$\frac{\rho_0}{\rho} = \frac{V_{\text{uc}}}{V_{\text{fiber}}} = \frac{2rLL}{\pi r^2 L} = \frac{2L}{\pi r}. \tag{8}$$

Kaganer's cylindrical model is now adapted to the trilobal fiber by introducing two different radius definitions, r_{middle} and r_{small}, as shown in Fig. 5. The radius r_{middle} is obtained by calculating it from the fiber's titer (e.g., dtex = 1 g/10,000 m) for the bulk density [1]. The radius r_{middle} is estimated to be 3/5th of the outer radius R. The radius r_{middle} represents the radius that is equivalent in the cross-sectional surface of cylindrical fibers. It is used to calculate the conductor-resistance R_{L} (Eq. 3).

The radius r_{small} is set to 1/5th of R, representing the curvature of the outer edge of one fiber arm which is needed to calculate the Hertzian contact-radius a_{ct} (Eq. 5). As a consequence, r_{small} strongly affects the contact resistance R_{ct} (Eq. 4). Moreover, the functional relationship among L, ρ, ρ_0, and the radius (Eq. 8) is modified for the new unit cell height $2R$ and the adequate fiber radius r_{middle}:

$$\frac{\rho_0}{\rho} = \frac{V_{\text{uc}}}{V_{\text{fiber}}} = \frac{2RL}{\pi r_{\text{middle}}^2}. \tag{9}$$

The effective thermal conductivity λ_{solid} is extremely sensitive to the ratio of the different radii. Therefore, images with a scanning electron microscope were taken (Fig. 2) for evaluation of r_{small} and r_{middle} to minimize this uncertainty and form the basis for Fig. 5.

In addition, the model is modified to the different possible fiber arrangements in the unit cell. The possible orientations of the trilobal fiber arms and their resulting number of contacts between each other are calculated for the case of two adjacent unit cells (assuming, there is at least one contact point at each fiber crossing), see Table 1.

The average force F on one fiber crossing has to be split according to the number of contacts. For this reason, building a unit cell for each possible arrangement $R_{\text{uc}}^{i\,\text{ct}}$ (number of contacts $i = 1, 2, 4$) and averaging these equally weighted values, a mean

Table 1 Possible number of contacts accounting for the trilobal cross section of the polyimide fiber, postulating at least one contact point at each fiber crossing

Number of fiber arms orientated to the ...				
Bottom of the upper unit cell	1	2	1	2
Top of the lower unit cell	1	1	2	2
Total number of contacts	1	2	2	4

total thermal resistance $R_{\mathrm{total,uc-mean}}$ was obtained:

$$R_{\mathrm{total,uc-mean}} = \frac{R_{\mathrm{uc}}^{1\mathrm{ct}} + 2R_{\mathrm{uc}}^{2\mathrm{ct}} + R_{\mathrm{uc}}^{4\mathrm{ct}}}{4}. \tag{10}$$

3 Calculation of the Total Thermal Conductivity

Starting from an additive model for the total thermal conductivity $\lambda_{\mathrm{total}}(T)$ of an evacuated insulation, there are only two contributions $\lambda_{\mathrm{solid}}(T)$ and $\lambda_{\mathrm{rad}}(T)$ to consider (Eq. 11). Gas conduction and related coupling effects do not exist as a result of the low gas pressure $p_{\mathrm{gas}} \leq 0.001\,\mathrm{hPa}$:

$$\lambda_{\mathrm{total}}(T) = \lambda_{\mathrm{solid}}(T) + \lambda_{\mathrm{rad}}(T). \tag{11}$$

The thermal conductivity $\lambda_{\mathrm{solid}}(T)$ of the solid is given by Eq. 7 and the contribution by radiation is given for $\lambda_{\mathrm{rad}}(T)$ by

$$\lambda_{\mathrm{rad}}(T) = \frac{16}{3}\frac{n^2\sigma T^3}{e\rho}, \tag{12}$$

where n is the effective refraction index, σ is the Stefan-Boltzmann constant, e is the specific extinction coefficient, and ρ is the sample density.

Other parameters that have to be taken into account are the external bearing load $p_{\mathrm{ext}} = 0.007\,\mathrm{MPa}$ and the specific extinction coefficient $e = 80\,\mathrm{m^2 \cdot kg^{-1}}$, derived by a plot of the experimentally determined thermal conductivity as a function of the third power of the temperature (Fig. 6). The specific extinction coefficient e is assumed to be a temperature-independent constant [8, 9]. The refraction index n is set equal to one, and the sample density is $\rho = 130\,\mathrm{kg \cdot m^{-3}}$. Other important material properties are the elastic modulus $E_{\mathrm{mod}} = 3\,\mathrm{GPa}$, Poisson's ratio $v = 0.4$, bulk density $\rho_0 = 1410\,\mathrm{kg \cdot m^{-3}}$, and the fiber's titer is 0.6 dtex (equals to $r_{\mathrm{middle}} \sim 3.7\,\mu\mathrm{m}$). Thermal-conductivity measurements were performed with a guarded hot-plate apparatus [10]. The relative measurement uncertainty is estimated to be 5 % for temperatures above 250 K and 10 % for temperatures below 150 K.

Figure 7 shows the measured thermal conductivity of the investigated polyimide specimen depicted as a function of temperature in comparison to the results of the cylindrical model and the trilobal model. Table 2 gives a listing of the single measurements of the mean thermal conductivity λ_{m} together with the boundary conditions. Here, for both models, the same bulk thermal conductivity λ_{bulk} (300 K) $\sim 0.153\,\mathrm{W \cdot m^{-1} \cdot K^{-1}}$

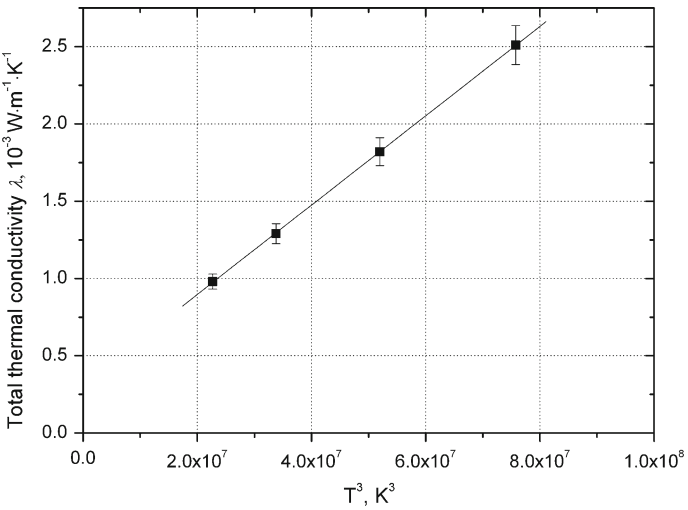

Fig. 6 Measurements of the thermal conductivity of the investigated polyimide specimen are depicted as a function of the third power of the temperature. The experimental results were obtained with a guarded hot-plate apparatus. In addition, a linear fit is added. The specific extinction coefficient $e = 80\,\mathrm{m}^2 \cdot \mathrm{kg}^{-1}$ can be derived from the slope (Eq. 12)

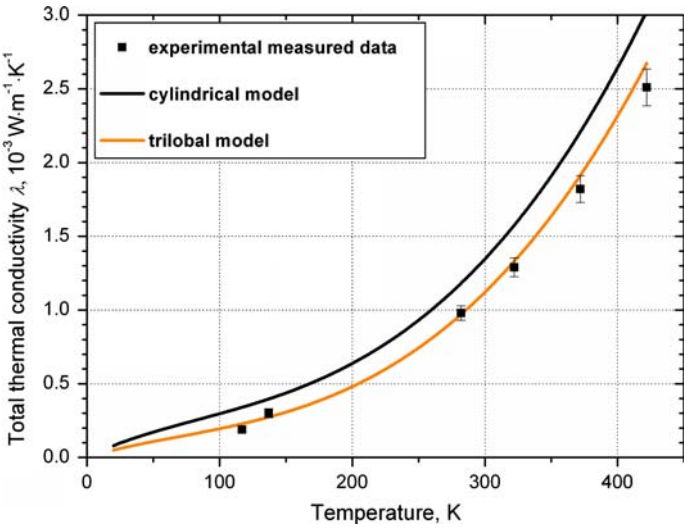

Fig. 7 Thermal conductivity of the investigated polyimide specimen is depicted as a function of temperature. Results of the cylindrical model and the trilobal model are compared to the experimental results of measurements with a guarded hot-plate apparatus

was used. Both theoretical models show the characteristic behavior, increasing slowly at low temperatures and faster at higher temperatures mainly due to radiation. The cylindrical model derives the highest values for the total thermal conductivity.

Unfortunately, the bulk thermal conductivity for the specimen could not be measured. In the literature, a wide band of thermal-conductivity values for polyimide

Table 2 Measurements of mean thermal conductivity λ_m and associated boundary conditions

T (K)	Mean thermal conductivity λ_m ($10^{-3}\,W\cdot m^{-1}\cdot K^{-1}$)	T_{cold} (K)	T_{hot} (K)
117.9	0.19	102.7	133
138.4	0.30	103.8	173
283	0.98	273	293
323	1.29	313	333
373	1.82	363	373
423	2.51	413	433

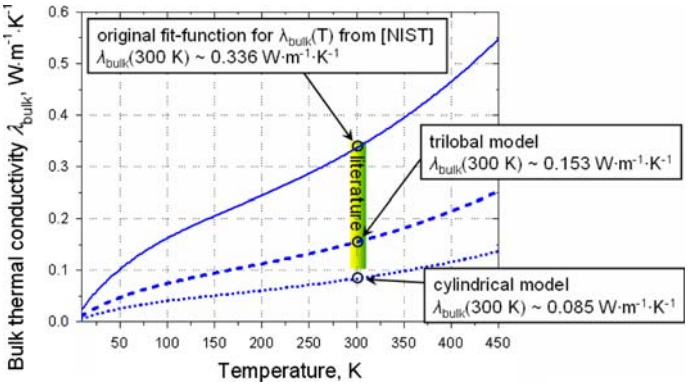

Fig. 8 Different bulk thermal conductivities λ_{bulk} for polyimide as a function of the temperature. Highest curve is a fit-function for polyimide taken from NIST [12]. To bring the trilobal model and measurements in good agreement, it was necessary to down-scale this fit-function by a factor of 0.45 (see middle curve). In addition, the necessary down-scaling by a factor of 0.25 for the cylindrical model is shown (see lowest curve); this results in a value at room temperature that is out of the band of thermal conductivities from the literature for polyimide at room temperatures (see shaded area) [11]

ranging from (0.1 to 0.35) $W\cdot m^{-1}\cdot K^{-1}$ at 300 K can be found [11]. This wide band could be a consequence of the anisotropy of the polymer orientation.

For calculations the thermal conductivity of the bulk material $\lambda_{bulk}(T)$ is being accounted for by using a fitting function from NIST (National Institute of Standards and Technology) [12]. This reference gives the only temperature-dependent thermal conductivity for bulk polyimide that could be found.

The numerical simulations for the trilobal model have shown that a value of approximately $0.153\,W\cdot m^{-1}\cdot K^{-1}$ for λ_{bulk} (300 K) fits best with the measured data. Hence, the temperature-dependent thermal conductivity function from NIST, $\lambda_{bulk,NIST}$ (300 K) $\sim 0.336\,W\cdot m^{-1}\cdot K^{-1}$, was downscaled accordingly for all temperatures.

Adjusting the thermal conductivity of the bulk material for the cylindrical model to fit the measured data leads to a bulk thermal conductivity λ_{bulk} (300 K) ~ 0.085 $W\cdot m^{-1}\cdot K^{-1}$. This value is lower than the values of bulk thermal conductivities known for polyimide, see Fig. 8. Obviously the cylindrical model neglects at least one important aspect, which can be assumed to be the very special non-cylindrical cross

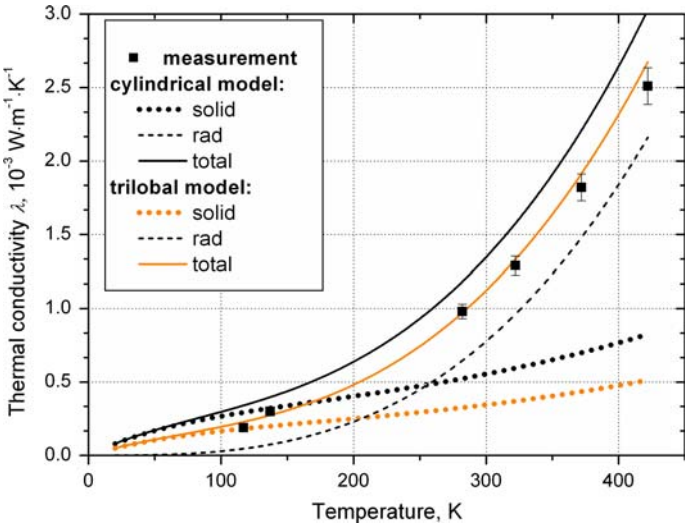

Fig. 9 Total thermal conductivity $\lambda_{\text{total}}(T)$ for the cylindrical model and the trilobal model as a function of temperature is shown. Total thermal conductivity is divided into its parts: λ_{solid} and λ_{rad}. In addition, measurements taken with a guarded hot-plate apparatus are displayed

section in this case. This supports that the trilobal model is a more realistic description of this special geometric situation.

Figure 9 shows the total thermal conductivity $\lambda_{\text{total}}(T)$ and their components $\lambda_{\text{solid}}(T)$ and $\lambda_{\text{rad}}(T)$ of the investigated polyimide specimen depicted as a function of temperature for the two models in comparison to the experimentally derived values. The contribution by radiation is calculated by Eq. 12 and is identical for both models. Moreover, it is worth mentioning that for lower temperatures ($T < 150\,\text{K}$) the thermal conductivity of the solid for the cylindrical model exceeds the measured values. The difference in the solid contribution is due to the adapted fiber model to the trilobal fiber cross section.

At high temperatures, the relative difference between the total thermal conductivity between the cylindrical and trilobal models is almost negligible due to the dominant radiation. Whereas, at low temperatures, the solid conductivity becomes dominant and the modification for the trilobal cross section of the polyimide fiber becomes obvious. The ratio of the solid thermal conductivity λ_{solid} for the cylindrical and trilobal models is a temperature-independent factor of approximately 1.61, which is due to the fact that $\lambda_{\text{bulk}}(T)$ is the only temperature-dependent variable in the relevant equation Eq. 6.

4 Conclusion

It could be shown that trilobal polyimide fibers provide a very low thermal conductivity due to their unique fiber form in combination with the low thermal conductivity of the bulk material. In comparison to other fiber insulations, this fiber is promising especially for cryogenic applications. Since this material has not been optimized for

thermal insulation applications so far, a significant potential for further improvement of the insulation properties seems likely.

Furthermore, Kaganer's cylindrical model was successfully adapted to this special cross section. It was shown that the contact resistance is the main factor for the total thermal conductivity which additionally strongly depends on the used fiber radius. Minimizing the contact area between two fibers maximizes the contact resistance, and therefore minimizes the thermal conductivity of the solid. Hence, the solid thermal conductivity is dominant for lower temperatures and explains the increasing relative difference between the cylindrical and trilobal models at lower temperatures. Neglecting the trilobal geometry would lead to errors of systematic deviation of about 60% with respect to the solid thermal conductivity.

Acknowledgments The scientific investigations have been carried out within the research project "icefuel®".[1] This joint research project started in July 2006 and is supported by the Bundesministerium für Bildung, Wissenschaft, Forschung und Technologie (BMBF), Federal Republic of Germany, in Bonn (FKZ 16SV2357). Furthermore, we gratefully acknowledge the support of Inspec Fibres (Evonic Indusries AG), who provided the SEM picture (Fig. 2).

References

1. H.L. Paul, K.R. Diller, J. Biomech. Eng. **125**, 639 (2003)
2. H. Bansemir, O. Haider, Cryogenics **38**, 51 (1998)
3. M.G. Kaganer, *Thermal Insulation in Cryogenic Engineering* (IPST Press, Jerusalem, 1969), pp. 18–25
4. A. Hofmann, Cryogenics **46**, 815 (2006)
5. D. Büttner, Ph.D. Thesis (University Würzburg, 1984)
6. C. Stark, Ph.D. Thesis (University Würzburg, 1991)
7. H. Hertz, J. Reine Angew. Math. **92**, 156 (1881)
8. J. Fricke, R. Caps, Int. J. Thermophys. **9**, 885 (1988)
9. VDI, *VDI-Wärmeatlas*, vol. 7 (Springer-Verlag, Berlin, 1994), pp. Kf1–Kf18
10. U. Heinemann, J. Hetfleisch, R. Caps, J. Kuhn, J. Fricke, *Proceedings of the Eurotherm Seminar N°44*, (Advances in Thermal Insulation, Espinho-Portugal, 1995), pp. 155–164
11. GoodFellow, *Polyimid (PI)—Physical Properties*, http://www.goodfellow.com/csp/active/static/G/Polyimid.html. Accessed 30 Aug 2007
12. National Institute of Standards and Technology (NIST), *Polyimid (PI)—Physical Properties*, http://cryogenics.nist.gov/MPropsMAY/Polyimide%20Kapton/PolyimideKapton_rev.htm. Accessed 30 Aug 2007

[1] State-of-the-art technology from different sectors included, icefuel® will develop a system for transport, storage, and conversion of energy, that is capable of buffering fluctuating peak load and supporting balance between power generation and power demand (for more information, see www.icefuel.de).